Phonon Raman scattering in $Y_{1-x}Pr_xBa_2Cu_4O_8$ ($x=0-1$) and $(Y_{1-x}Pr_x)_2Ba_4Cu_7O_{15-\delta}$ ($x=0-0.6$)

M. Käll
Department of Physics, Chalmers University of Technology, S-412 96 Göteborg, Sweden

A. P. Litvinchuk
Institut für Festkörperphysik, Technische Universität Berlin, Sekr. 5-4, Hardenbergstrasse 36, D-106 23 Berlin, Federal Republic of Germany

P. Berastegui and L.-G. Johansson
Department of Inorganic Chemistry, Chalmers University of Technology, S-412 96 Göteborg, Sweden

L. Börjesson
Department of Physics, The Royal Institute of Technology, S-100 44 Stockholm, Sweden

M. Kakihana and M. Osada
Research Laboratory of Engineering Materials, Tokyo Institute of Technology, 4259 Nagatsuta, Midori-ku, Yokohama 227, Japan
(Received 30 June 1995)

We report on a Raman-scattering investigation of phonons in ceramic $Y_{1-x}Pr_xBa_2Cu_4O_8$ ($Y_{1-x}Pr_x124$) with $x=0-1$, and $(Y_{1-x}Pr_x)_2Ba_4Cu_7O_{15-\delta}$ ($Y_{1-x}Pr_x247$) with $x=0-0.6$. It is found that the A_g symmetry phonons of the BaO layers and the CuO double-chain layers increase in frequency with Pr content x, while B_{2g} and B_{3g} symmetry phonons decrease in frequency. In the $Y_{1-x}Pr_x247$ samples we are able to identify two symmetry allowed apical oxygen A_g modes. The B_{1g}-like plane oxygen phonon softens by $\sim 12\%$ from $x=0$ to $x=1$, and exhibits a two-mode behavior at intermediate x in both $Y_{1-x}Pr_x124$ and $Y_{1-x}Pr_x247$. Polarized micro-Raman spectra of Pr124 crystallites show that several phonons are asymmetric, exhibiting Fano line shapes similar to what has been found in superconducting Y124. The variation in phonon frequencies with Pr content is similar to what has been reported for the single-chain cuprate $Y_{1-x}Pr_xBa_2Cu_3O_{7-\delta}$ ($Y_{1-x}Pr_x123$), and the changes can be understood from the variation in structural parameters. We do not observe any peculiarities that can explain the disappearance of superconductivity, or the different rates of T_c suppression in the three different Y-Ba-Cu-O systems, upon Pr substitution.

I. INTRODUCTION

Among the various isomorphic substitutions possible in the $YBa_2Cu_4O_7$ high-T_c superconductor, the substitution of Pr for Y has received the most attention (for a review see Ref. 1). The reason for this interest is that $Y_{1-x}Pr_xBa_2Cu_3O_7$ ($Y_{1-x}Pr_x123$) becomes semiconducting at $x\approx 0.55$, while T_c remains at ~ 90 K when other rare-earth elements are substituted for Y. Despite the large number of experimental and theoretical reports on the $Y_{1-x}Pr_x123$ system the negative effect that Pr has on superconductivity is still not completely understood. The fact that $PrBa_2Cu_3O_7$ is semiconducting and that doping with Ca^{2+} yields superconducting $Pr_{1-y}Ca_yBa_2Cu_3O_7$ with T_c as high as 47 K for $y=0.5$ (Ref. 2) indicates that the effective valence of Pr is higher than $+3$, i.e., Pr fills or localizes the mobile holes responsible for superconductivity. These experimental observations are well accounted for in a recent model by Fehrenbacher and Rice.[3] They argue that Pr123 is the only $R123$ structure where it is energetically more favorable for a doped hole to reside in a local R IV state, composed of a mixture of R^{4+} ($4f^1$) and $R^{3+}+$O-ligand hole ($4f^2\underline{L}$) states, than in the CuO_2-plane conduction band dominated by hybridized Cu $3d$ and O $2p$ orbitals. In this picture the only significant charge transfer that occurs when Pr is substituted for Y takes place within the CuO_2-Pr/Y-CuO_2 layers, while the CuO chains have a constant hole concentration in accordance with optical measurements.[4] In this context it is notable that Pr has been found to be much less effective in suppressing superconductivity in the $Y_{1-x}Pr_xBa_2Cu_4O_8$ ($Y_{1-x}Pr_x124$) and $(Y_{1-x}Pr_x)_2Ba_4Cu_7O_{15}$ ($Y_{1-x}Pr_x247$) systems, which contain CuO_2-Pr/Y-CuO_2 layers almost identical to $Y_{1-x}Pr_x123$. In $Y_{1-x}Pr_x124$ superconductivity persists up to $x\geqslant\sim 0.8$ and Pr124 has recently been found to be metallic below room temperature.[5–7] It is likely that an explanation of the differences with respect to $Y_{1-x}Pr_x123$ will involve the extra CuO units present in the 124 and 247 compounds. The 124 structure contains double CuO chains,[8] while the 247 structure can be seen as a periodic intergrowth of 123 and 124 unit cells, i.e. the structure contains both single and double chains in equal proportions. One possibility could be that the double chains provide additional holes that counteract the hole-filling/localization effect of Pr doping, i.e. the charge transfer associated with Pr substitution for Y would also involve the CuO chain region. One way to detect such charge-transfer effects is to investigate the change in the phonon spectrum as a function of doping.

A number of Raman scattering studies on oxygen-deficient and isomorphically substituted $R123$ have shown that the optical phonons are sensitive to changes in the internal charge distribution and bond distances.[9] Radousky *et al.*[10] investigated the frequency changes of the symmetric c axis (A_g symmetry) phonons in $Y_{1-x}Pr_x123$ with x and made a comparison with data for various superconducting $R123$.[11] It was found that the A_g phonon frequencies scaled with the average size of the R ion in both $Y_{1-x}Pr_x123$ and $R123$, if a Pr radius corresponding to a $+3$ valence was assumed. Iliev *et al.*[12] found similar changes for phonons of B_{2g} and B_{3g} symmetry, i.e., for vibrations along the a and b axis, respectively. These results indicate that the change in the $Y_{1-x}Pr_x123$ phonon spectrum with x is mainly due to changes in the internal bond distances. Yang and co-workers,[13–15] however, have argued that the hardening of the apical oxygen and Ba A_g modes with x is a signature of a hole transfer to the Ba site.

Considerable attention has been given to the temperature dependence of the plane-oxygen out-of-phase bending A_g mode, since this phonon displays pronounced renormalization effects at T_c in superconducting $R123$ (Ref. 16) but exhibit a normal temperature dependence in nonsuperconducting Pr123 (Ref. 17). While the renormalization at T_c rapidly disappears with Pr substitution, it has been found that the plane-oxygen bending mode is extremely broad for intermediate x.[18] If this broadening is indicative of a two-mode behavior, i.e., a splitting into ''Y-like'' and ''Pr-like'' modes, or phase segregation is a matter of debate.[13,18,19] There are also several Raman-scattering reports on Y123/Pr123 superlattices.[20–22] In general, it has been found that the phonon spectrum for such structures is very similar to a superposition of the spectra for the isolated pure phases, indicating a weak coupling along the c axis. In the case of $Y_{1-x}Pr_x124$ we are aware of only two preliminary Raman scattering reports by Watanabe and co-workers,[23,24] covering the range $x=0-0.6$.

Here we report on a Raman-scattering investigation of phonons in ceramic $Y_{1-x}Pr_xBa_2Cu_4O_8$ ($Y_{1-x}Pr_x124$) with $x=0-1$ and $(Y_{1-x}Pr_x)_2Ba_4Cu_7O_{15-\delta}$ ($Y_{1-x}Pr_x247$) with $x=0-0.6$ at room temperature and at $T=20$ K. The variation in B_{2g}, B_{3g}, and A_g symmetry phonon frequencies with x is discussed in relation to changes in the structural parameters and compared with previous reports on the single-chain material. We investigate polarized micro-Raman spectra of single-crystallites in Pr124 and compare the phonon line shapes with what has been found in superconducting Y124.

II. SAMPLE PREPARATION AND CHARACTERIZATION

A series of polycrystalline samples with nominal composition $Y_{1-x}Pr_xBa_2Cu_4O_8$ ($x=0-0.8$) and $(Y_{1-x}Pr_x)_2Ba_4Cu_7O_{15-\delta}$ ($x=0-0.6$) were prepared by a polymerized-complex method described in Refs. 25 and 26. One polycrystalline $PrBa_2Cu_4O_8$ sample was prepared by a solid-state reaction procedure according to Ref. 6.

The purity of the samples was checked through the Raman measurements as well as with the Guinier technique, using Cu $K\alpha_1$ radiation with Si as an internal standard. Small amounts of crystalline impurities, in particular $BaCuO_2$ (1–3 %, irrespective of x) were found in the mixed

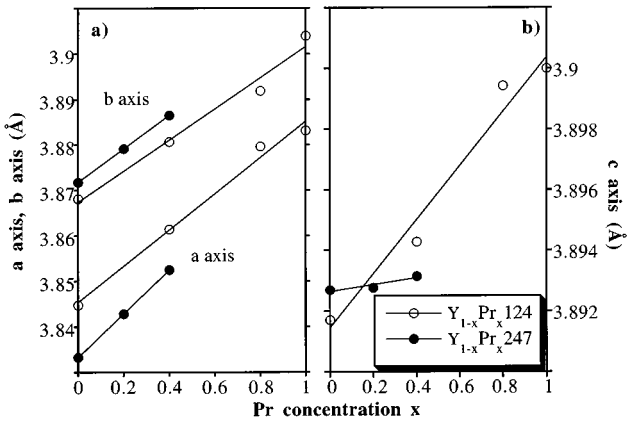

FIG. 1. (a) a and b axis vs x in $Y_{1-x}Pr_x124$ (open circles) and $Y_{1-x}Pr_x247$ (solid circles). (b) c axis/7 in $Y_{1-x}Pr_x124$ (open circles) and c axis/13 in $Y_{1-x}Pr_x247$ (solid circles).

$Y_{1-x}Pr_x124$ samples. The amount of $BaCuO_2$ in the $Y_{1-x}Pr_x247$ samples increased with x up to $\sim 5\%$ for the $x=0.6$ sample. The Pr124 sample contained traces of $BaPrO_3$ and $BaCuO_2$ ($<1\%$ in total).

The variation of lattice parameters and interatomic distances with x were investigated by neutron and x-ray-diffraction measurements on selected samples. Details of these investigations for the $Y_{1-x}Pr_x124$ ($x=0$, 0.2, 0.4, 0.6, and 0.8) samples can be found in Ref. 27. The neutron-diffraction results on the $Y_{1-x}Pr_x247$ ($x=0,0.2,0.4$) samples will be presented elsewhere (a preliminary report is given in Ref. 28).

Figure 1 shows the evolution of the lattice parameters with increasing x for $Y_{1-x}Pr_x124$ ($x=0-0.8$, neutron-diffraction results[27]), $Y_{1-x}Pr_x247$ ($x=0-0.4$, neutron-diffraction results[28]) and Pr124 (x-ray-diffraction results). The a and b axes were found to increase continuously with x in both $Y_{1-x}Pr_x124$ and $Y_{1-x}Pr_x247$, as has been found in $Y_{1-x}Pr_x123$.[1] In the $Y_{1-x}Pr_x124$ series the c axis increases slightly with x, similar to what has been observed in $Y_{1-x}Pr_x123$,[1] while the $Y_{1-x}Pr_x247$ samples have a more or less constant c axis, irrespective of x.

The oxygen contents of the samples were checked by the iodometric titration method as well as by refinements of the chain-oxygen occupation factors from the neutron-diffraction measurements. The oxygen deficiency of the $Y_{1-x}Pr_x124$ samples was found to be ~ 0.05, irrespective of x, while the $Y_{1-x}Pr_x247$ samples exhibited a slightly increasing oxygen deficiency with x, from $\delta \approx 0.07$ for $x=0$ to $\delta \approx 0.2$ for $x=0.4$.

The superconducting properties of the $Y_{1-x}Pr_x247$ samples were investigated by measuring the temperature dependent magnetic response of the samples with the ac susceptibility technique. All samples were found to be superconducting; the width of the superconducting transitions was found to increase somewhat with x. The $Y_{1-x}Pr_x124$ samples were investigated by the usual four-probe resistivity technique. All samples up to and including $x=0.8$ were found to be superconducting, with transition widths only marginally larger than in the pure Y124 sample.[27] In Fig. 2 we show $T_{c,\mathrm{onset}}$ for the $Y_{1-x}Pr_x247$ and $Y_{1-x}Pr_x124$ samples from the present work, together with data for

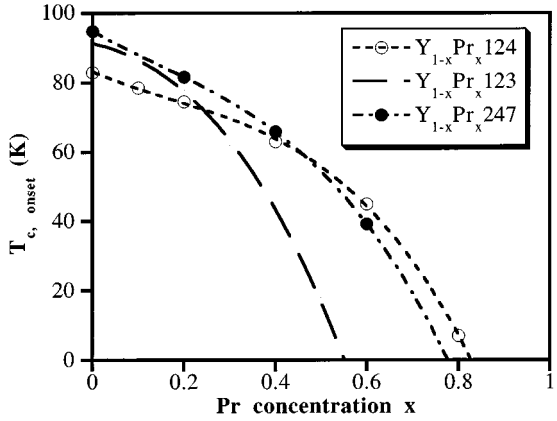

FIG. 2. T_c vs x in $Y_{1-x}Pr_x124$ (open circles) and $Y_{1-x}Pr_x247$ (solid circles) together with fits to a third-order polynomial as a guide to the eye. The long-dashed curve indicate the trend in T_c vs x for $Y_{1-x}Pr_x123$ taken from data compiled by Radousky (Ref. 1).

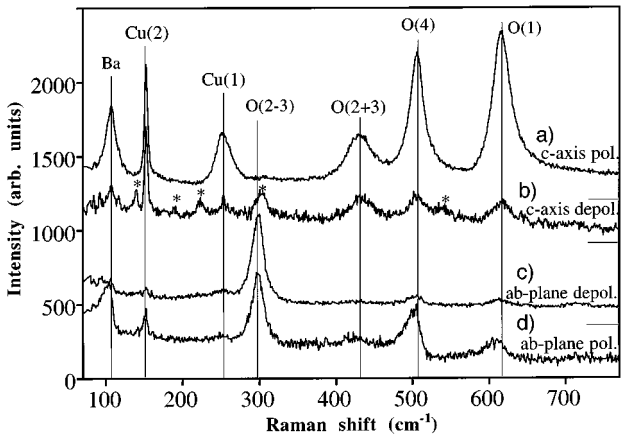

FIG. 3. Polarized and depolarized micro-Raman spectra of Pr124 crystallites at room-temperature. A_g symmetry phonons are marked with vertical lines and assignments according to Ref. 29. Peaks assigned to B_{2g}/B_{3g} symmetry phonons are marked by stars in the c-axis depolarized spectrum. The intensity scale of this spectrum have been multiplied by two. The base-lines for each spectrum are marked by horizontal lines.

$Y_{1-x}Pr_x123$ compiled by Radousky[1] as a comparison.

III. EXPERIMENT

Raman-scattering measurements were performed in the frequency range 70–800 cm^{-1} using the 514.5-nm line of an argon laser for excitation. The scattered light was dispersed by a SPEX 1877 triple spectrometer and detected by a liquid-N_2-cooled CCD camera. The slits of the spectrometer were set to give a resolution of ~ 4 cm^{-1}. Unpolarized low-temperature measurements were performed in a near-backscattering geometry using ~ 4 mW of incident radiation focused to a ~ 50-μm-diam spot, with the samples mounted on the cold finger of a liquid-He cryostat. Room-temperature measurements were made in backscattering geometry using a $100\times$, $NA = 0.95$, microscope objective for focusing and collection. The laser-spot size was in this case ~ 2 μm in diameter. For the Pr124 sample we were able to obtain polarized spectra of individual large crystallites embedded in the ceramic matrix. This was not possible for the samples prepared by the polymerized-complex method, since the crystallites were too small, typically < 1 μm in diameter.

IV. RESULTS AND DISCUSSION

A. Polarized Raman spectra of Pr124

In Fig. 3 we show polarized and depolarized micro-Raman spectra of Pr124 recorded at room temperature and corrected for the Bose factor $[1+n(\omega,T)]$. A phonon symmetry analysis of Pr124 yields the same number of Raman active vibrations as for the isostructural Y124 superconductor (see, e.g., Ref. 29), namely, $6(A_g+B_{2g}+B_{3g})$ modes. Spectrum (a) in Fig. 3 was obtained from the edge of a crystallite oriented with the c axis parallel to the incident and scattered polarization vectors. This c-axis polarized measurement selects the α_{zz} components of the polarizability tensors for the A_g-symmetry modes. Following Heyen *et al.*,[29] the observed phonons are expected to be dominated by symmetric c-axis vibrations of Ba at ~ 107 cm^{-1}, Cu(2) at ~ 151 cm^{-1}, Cu(1) at ~ 251 cm^{-1}, O(2)+O(3) in phase at ~ 430 cm^{-1}, O(4) at ~ 506 cm^{-1}, and O(1) at ~ 614 cm^{-1}.

Spectrum (b) of Fig. 3 shows a c-axis depolarized measurement of the crystallite investigated in spectrum (a), i.e., the incident light is polarized along the c axis, while the scattered light with polarization within the ab plane is analyzed. In this case phonons of B_{2g} and B_{3g} symmetry are visible, in addition to the A_g modes, which occur because of "polarization leakage." From a comparison with the single-crystal investigations of Y124,[29] Y123,[30] and $Y_{1-x}Pr_x123$,[12] we may assign the weak peaks marked by asterisks in Fig. 3(b) to B_{2g} and B_{3g} modes of Pr124. The ~ 223-cm^{-1} and ~ 303-cm^{-1} phonons can be followed as a function of x in $Y_{1-x}Pr_x124$ (see Sec. IV B below). In Y124 they have been assigned to the O(1) B_{2g} and the Cu(1) B_{3g} modes, respectively.[29] The weak peaks at ~ 190 and ~ 540 cm^{-1} occur at similar frequencies as Pr123 phonons assigned to O(4) B_{2g} and O(2/3) B_{2g}/B_{3g} modes, respectively.[12] In Y124 we reproducibly observe an analogous pair of modes at ~ 210 cm^{-1} and at ~ 554 cm^{-1},[31] at similar frequencies as the O(4) B_{2g} and O(2/3) B_{2g}/B_{3g} modes in Y123.[30] We also observe a weak peak at ~ 140 cm^{-1} in Fig. 3(b), which may be because of a superposition of Cu(2) B_{2g} and B_{3g} motion. These modes have been reported at ~ 130–140 cm^{-1} in $Y_{1-x}Pr_x123$.[12,30]

Spectra (c) and (d) of Fig. 3 are ab-plane depolarized and polarized measurements, respectively, of a crystallite oriented with the c axis directed along the incident laser beam. These spectra also select A_g-symmetry phonons, but now combinations of the α_{xx} and α_{yy} components of the polarizability tensor are recorded. The intense peak at ~ 298 cm^{-1} in the (c) spectrum can be assigned to the O(2)-O(3) out-of-phase A_g phonon, since the approximate B_{1g} symmetry (in tetragonal notation) of this mode[29] yields a large depolarized intensity. In the following we refer to this mode as the O(2/3) "B_{1g}" mode. In Table I we summarize the phonon

TABLE I. Phonon frequencies at room-temperature for Pr124 and Y124 (this work) together with data for Pr123 and Y123 from Radousky *et al.* (Ref. 10).

cm^{-1}	ω_{Y124}	ω_{Pr124}	ω_Y-ω_{Pr}	ω_{Y123}	ω_{Pr123}	ω_Y-ω_{Pr}
Ba A_g	101	107	+6	119	129	+9
Cu(2) A_g	149	151	+2	151	149	−2
Cu(1) A_g	248	251	+3	Not active	Not active	Not active
O(2/3) B_{1g}	339	298	−41	340	298	−42
O(2+3) A_g	433	430	−3	~440	~430	−10
O(4) A_g	496	506	+10	503	516	+13
O(1) A_g	600	614	+14	Not active	Not active	Not active
O(1) B_{2g}	239	223	−16	Not active	Not active	Not active
Cu(1) B_{3g}	313	303	−10	Not active	Not active	Not active

frequencies of Pr124 at room temperature, obtained from the spectra in Fig. 3, together with data for Y123, Pr123, and Y124 as a comparison. The variation in phonon frequencies between the different cuprates are discussed below.

In the ab-plane polarized spectrum [Fig. 3(d)] we find that the Ba, O(4),and O(1) phonons are clearly asymmetric, indicating a substantial coupling between these A_g-symmetry modes and the continuum scattering in this polarization geometry. The asymmetric phonon line shapes are well described by the Fano function:[16]

$$I(\omega)\sim[q+(\omega-\omega_p)/\Gamma]^2/[1+(\omega-\omega_p)^2/\Gamma^2],$$

where ω_p and Γ are the frequency and half-width, respectively, of the renormalized phonon, and q is inversely proportional to the degree of line-shape asymmetry. The asymmetry is most pronounced for the Ba and O(4) modes, which can be fitted with $(q;\Gamma)\approx(-2;\ 7\ cm^{-1})$ and $(-3;\ 10\ cm^{-1})$, respectively, with frequencies ω_p the same as those obtained by fitting the c-axis polarized spectrum with Lorentzian line shapes. The O(1) mode is found to be asymmetric in both the ab-plane polarized spectrum ($q\approx-4$) and in the c-axis polarized spectrum ($q\approx12$) with $(\omega_p;\Gamma)\approx(614\ cm^{-1};\ 14\ cm^{-1})$ in both scattering geometries.

The microscopic origin of the Fano-type phonon asymmetries in the cuprates is not well understood. For the Y123 superconductor, the pronounced Fano shape of the O(2/3) "B_{1g}" phonon[16] has been interpreted as the result of a phonon modulation of electronic interband transitions that involve the CuO_2-plane conduction band.[32–34] In this case, one would expect that the phonon asymmetry (i.e., the q parameter) would be sensitive to a change in the electronic state of the CuO_2 planes. Indeed, the degree of B_{1g} phonon asymmetry in Y123 decreases rapidly with increasing oxygen deficiency,[35,36] an effect that may be linked with the decreasing number of carriers in the CuO_2 planes. In this respect it is interesting to note that the O(2/3) B_{1g} phonon is symmetric in both Y124,[29] which has a low carrier concentration compared to Y123, and in nonsuperconducting Pr123,[17] where the CuO_2-plane carriers presumably are localized.[3] As expected from a comparison with the latter compounds, we find from Fig. 3(c) that the O(2/3) B_{1g} phonon is symmetric in Pr124.

The Fano shapes of the Ba, O(4), and O(1) A_g phonons in the ab-plane polarized spectrum of Pr124 are remarkably similar to what has been reported for superconducting Y124.[37] If one assumes that the mechanism that gives rise to the asymmetric shapes of these phonons is of the same type as has been suggested for the O(2/3) B_{1g} phonon in Y123, this similarity suggests that the phonons in question couple to parts of the Fermi surface that are only weakly affected by the replacement of Pr for Y, and the loss of superconductivity. In this context it is interesting to note that optical reflectivity spectra of untwinned Pr123 by Takenaka *et al.*[4] showed that the effective carrier density in the CuO chains was the same as in superconducting Y123, while the optical response of the CuO_2 layers was similar to oxygen-deficient insulating Y123. While there are no polarized optical measurements of Pr124 as yet, recent results on Y124 by Basov *et al.*[38] show that the double CuO chains are highly conducting, and even accommodate a significant portion of the superconducting condensate. In view of these observations, it is natural to suggest that the Ba, O(4), and O(1) A_g phonons mainly couple to interband transitions that involve the CuO chain bands, and that these bands are very similar in Pr124 and Y124.

B. Raman active phonons in Pr substituted Y247 and Y124

Figures 4(a) and 4(b) show representative unpolarized Raman spectra of the $Y_{1-x}Pr_x124$ and $Y_{1-x}Pr_x247$ series, respectively, at $T=300$ K. The seven A_g symmetry c-axis vibrations described in the preceding paragraph also dominate the $Y_{1-x}Pr_x247$ spectra; the major difference with respect to $Y_{1-x}Pr_x124$ spectra being the intensity of the Cu(1) and O(1) modes, which is proportional to the density of the double chains in the two structures. The presence of $BaCuO_2$ is revealed through its strongest peak at ~630 cm^{-1} [see spectrum included in Fig. 4(b)].

We have also investigated the temperature dependence of the phonon parameters for some of the $Y_{1-x}Pr_x124$ samples. For low Pr content, $x\leqslant0.2$ we observe superconductivity-related phonon frequency and line-width anomalies that are similar to what has been reported for pure Y124.[31,37] The effects are found to decrease continuously with x and disappear at $x=0.3$–0.4. We do not find any evidence for a shift of the superconducting gap with increasing x and decreasing

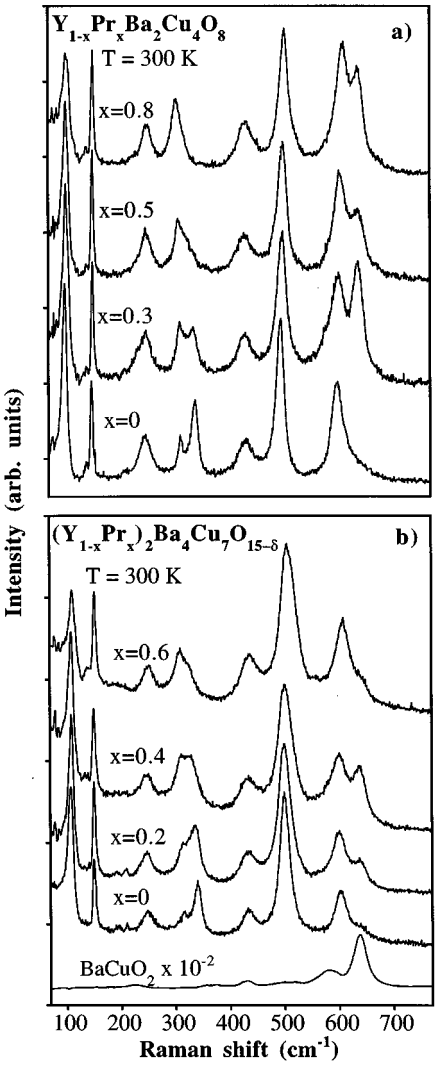

FIG. 4. (a) Micro-Raman spectra of $Y_{1-x}Pr_x124$ and (b) $Y_{1-x}Pr_x247$ and $BaCuO_2$ recorded at room temperature.

T_c, as has recently been claimed by Watanabe *et al.*[24] These results will be described in detail elsewhere.

1. Double CuO-chain modes

The double-chain vibrations in $Y_{1-x}Pr_x124$ and $Y_{1-x}Pr_x247$ are particularly interesting, since chain modes are Raman forbidden in $Y_{1-x}Pr_x123$ because of the inversion symmetry of the single chains. Figure 5 shows the frequency variation of the Cu(1) and O(1) modes as a function of x in $Y_{1-x}Pr_x124$ and $Y_{1-x}Pr_x247$ at $T=20$ K. The O(1) B_{2g} mode occurs at the same frequency in Y247 as in Y124. The intensity of this mode is, however, lower in Y247, and we could not identify it with certainty in the doped samples. We also could not positively identify the Cu(1) B_{3g} mode in the unpolarized measurements of Pr124 at $T=20$ K, as it occurs at almost exactly the same frequency as the intense O(2/3) B_{1g} mode (see Table I). If we assume that the temperature-induced hardening of the Cu(1) B_{3g} mode is the same as in Y124 (i.e., ~ 2 cm^{-1}), we expect it to occur at ~ 305 cm^{-1}, in good agreement with the trend shown in Fig. 5.

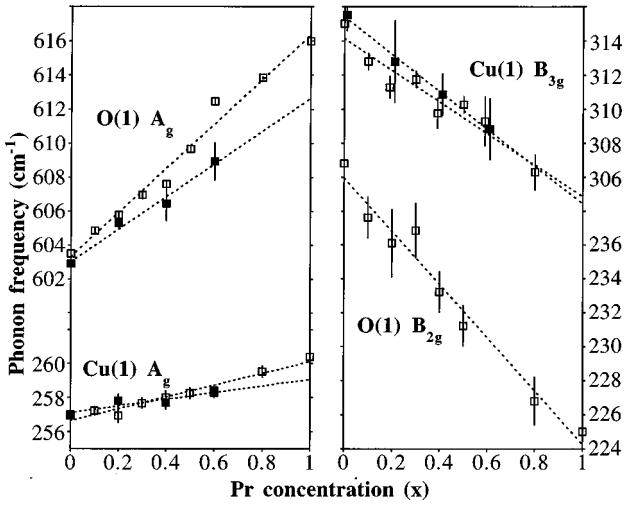

FIG. 5. Frequencies of the Cu(1) and O(1) double-chain modes in $Y_{1-x}Pr_x124$ (open symbols) and $Y_{1-x}Pr_x247$ (closed symbols) at $T=20$ K.

As can be seen in Fig. 5, none of the chain vibrations exhibit any anomalies in their composition dependence that can be associated with the disappearance of superconductivity. In the 124, 247, and 123 systems the substitution of the larger Pr ion [radius $r(Pr^{3+})\approx 1.12$ Å] for the smaller Y^{3+} ion ($r\approx 0.9$ Å) yields an expansion of the a and b axes. This is expected to result in a weakening of the force constants in the x and y directions, which would explain the decrease of the B_{2g} and B_{3g} phonon frequencies with x. The large Pr ion also gives rise to an increase of the CuO_2 plane-plane distance. This expansion along the c axis is, however, almost completely compensated for by a contraction of the plane–CuO-chain distance and, in the case of the 124 and 247 systems, by a contraction of the chain-chain distance.[27] It is likely that the hardening of the A_g c-axis vibrations of the double-chain layers with increasing x is because of this bond-length contraction.

It should be noted that the apical-oxygen O(4) B_{3g} mode in $Y_{1-x}Pr_x123$ [$\omega\approx 303$–310 cm^{-1} for $x=0$ (Refs. 12 and 30)] exhibits roughly the same concentration dependence as the chain-copper Cu(1) B_{3g} mode in $Y_{1-x}Pr_x124$ (see Table I). The assignment of the 313-cm^{-1} line in Y124 and Y247 to a double CuO-chain vibration was based on the fact that the intensity of this mode is higher in Y124 than in Y247, which contains half as many double chains.[29] An alternative interpretation could be that the line around 310 cm^{-1} is caused by the O(4) B_{3g} mode in all the Y-Ba-Cu-O structures, but that the polarizability is enhanced by the presence of the double chains.

2. BaO-plane phonons

The compression of the region between the CuO_2 planes and the CuO chains along the c axis when Pr is substituted for Y is reflected in a hardening of the O(4) and Ba A_g modes in the 124 as well as in the 123 system. This hardening is, however, $\sim 25\%$ smaller in the 124 system than in 123 for

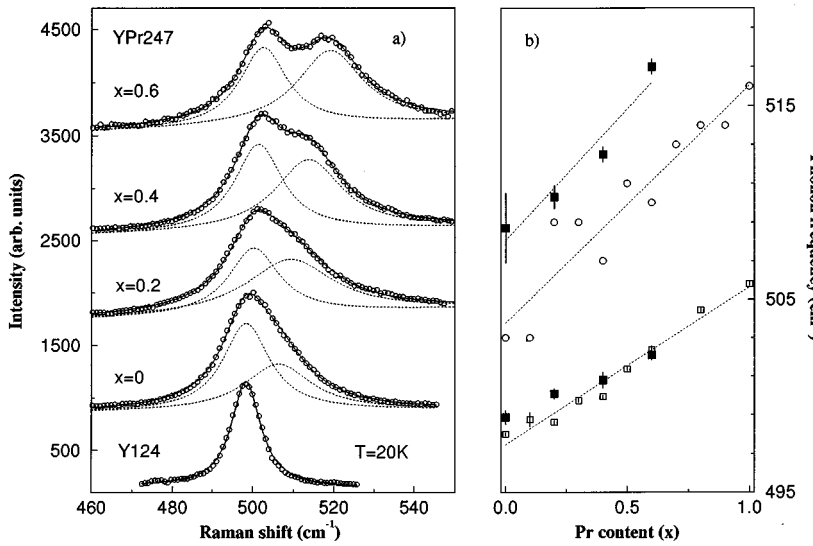

FIG. 6. (a) Apical oxygen O(4) A_g modes in $Y_{1-x}Pr_x247$ and Y124 at $T=20$ K, together with fits to Lorentzian line shapes. (b) Frequencies of the O(4) modes in $Y_{1-x}Pr_x124$ (open squares) and $Y_{1-x}Pr_x247$ (filled squares) at $T=20$ K together with data for the O(4) mode in $Y_{1-x}Pr_x123$ at $T=300$ K (circles) reported by Radousky *et al.* (Ref. 10).

both the O(4) and the Ba A_g modes (see Table I). In the 123 system the expansion of the CuO_2 plane-plane distance along the *c* axis induced by the large Pr ion causes an ''internal pressure'' on the BaO-plane region only, while in the 124 system it is distributed over both the double-chain region and the BaO-plane region. This structural difference then naturally explains why the BaO-plane A_g phonons exhibit a slower frequency increase in 124 than in 123 with Pr substitution.

We should note that the very high values of the O(4) A_g-mode frequency that have been found in some Raman investigations of Pr123 [up to $\omega_{O(4)}\approx 525$ cm^{-1} (Refs. 12, 13, 19, 20, 22, and 39)] seems to be caused by Pr substitution *on the Ba site*.[40] Ren *et al.*[40] measured $\omega_{O(4)}\approx 527$ cm^{-1} for $Pr_{1.25}Ba_{1.75}Cu_3O_7$ but $\omega_{O(4)}\approx 514$ cm^{-1} for fully oxygenated Pr123, i.e., similar to the value reported by Radousky *et al.*[10]

The $Y_{1-x}Pr_x247$ structure contains two crystallographically distinct apical oxygen sites, one of them, $O(4)_{124}$, close to the double CuO chains and the other, $O(4)_{123}$, close to the single CuO chains. Both of these sites have $C^z{}_{2v}$ symmetry and should therefore contribute one Raman-active A_g mode each.[29] The $T=20$ K spectra of Fig. 6(a) reveals that the spectral region around 500 cm^{-1} in $Y_{1-x}Pr_x247$ indeed contains two Lorentzian phonons. In Fig. 6(b) we have plotted the frequency of these two modes as a function of *x* together with the $O(4)_{124}$ frequency in $Y_{1-x}Pr_x124$ at $T=20$ K. We have also included $O(4)_{123}$ frequency data for $Y_{1-x}Pr_x123$ (at $T=300$ K) reported by Radousky *et al.*[10] By comparing the position and *x* dependence of the two $Y_{1-x}Pr_x247$ modes with the O(4) modes in $Y_{1-x}Pr_x124$ and $Y_{1-x}Pr_x123$ it is evident that the low-frequency phonon in $Y_{1-x}Pr_x247$ is caused by the $O(4)_{124}$ A_g mode, while the high-frequency phonon can be assigned to the $O(4)_{123}$ A_g mode. Figure 6(a) also shows that the intensity of the $O(4)_{123}$ mode relative to the $O(4)_{124}$ mode is increasing with *x*. This could be caused by a change in the polarizability of the Cu(1)—O(4)—Cu(2) bonds caused by, e.g., the slightly increasing oxygen deficiency with *x* in $Y_{1-x}Pr_x247$ or by a small Pr^{3+} substitution for Ba^{2+} as discussed above; the increasing amount of $BaCuO_2$ (see Sec. II) and the slower increase in the *c*-axis length with *x* (see Fig. 1) in $Y_{1-x}Pr_x247$ compared to $Y_{1-x}Pr_x124$ may point in the latter direction.

The $Y_{1-x}Pr_x247$ structure also contains two distinct Ba sites, which should contribute one A_g mode each. We are, however, not able to reliably decompose the frequency region around the Ba mode(s) into two peaks, even at $T=20$ K. If the $Y_{1-x}Pr_x247$ spectra are fitted with one line, we find that the frequency and linewidth (HWHM) increase from $(\omega_p,\Gamma)\approx(109\ \text{cm}^{-1},\ 4\ \text{cm}^{-1})$ at $x=0$ to $(114\ \text{cm}^{-1},\ 6\ \text{cm}^{-1})$ at $x=0.6$ (at $T=20$ K). Both the absolute frequency and the compositional dependence are thus intermediate between $Y_{1-x}Pr_x124$ and $Y_{1-x}Pr_x123$ (see Table I). In $Y_{1-x}Pr_x124$ we find that the linewidth of the Ba phonon is more or less independent of *x* and that the frequency changes smoothly between the endpoint values. It is thus possible that the increasing linewidth of the ''Ba mode'' in $Y_{1-x}Pr_x247$ is a result of a superposition of two modes with slightly different *x* dependencies, as was the case for the apixal oxygen modes discussed above.

3. CuO_2 plane phonons

Table I shows that the frequency shifts of the CuO_2-plane A_g modes when Pr is exchanged for Y are very similar in the 124 and the 123 structures. This is not surprising, since the main structural difference between the two systems is caused by the CuO chains, which are far from the CuO_2 planes. The large softening of the O(2/3) B_{1g} phonon by more than 10% can be understood as the result of the large increase in the available volume[27] around the plane-oxygen ions. The Cu(2) line should also soften because of the expansion of the CuO_2-plane region, but this effect seems to be completely compensated by the contraction of the Cu(2)-O(4) bond length. The only phonon that we find puzzling given the structural changes described above is the A_g phonon at ~ 430 cm^{-1}. The very small softening of this phonon compared to the O(2/3) B_{1g} mode indicates that the ~ 430-cm^{-1} phonon may not be a pure O(2)+O(3) in-phase A_g mode. One possibility is that it contains some O(4) *c*-axis motion, as such a mixing would tend to reduce the effect of

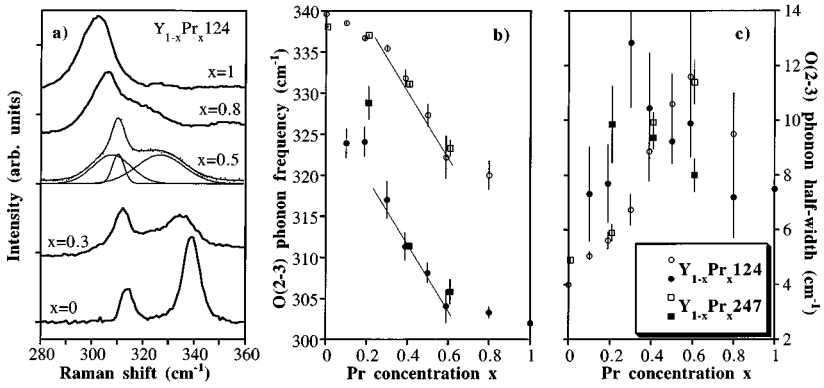

FIG. 7. (a) The frequency region around the plane-oxygen O(2–3) B_{1g} and double-chain Cu(1) B_{3g} phonons for $Y_{1-x}Pr_x124$ at $T=20$ K. (b) The frequency of the Y-like (open symbols) and Pr-like (filled symbols) O(2–3) B_{1g} modes in $Y_{1-x}Pr_x124$ (circles) and $Y_{1-x}Pr_x247$ (squares) at $T=20$ K. (c) Linewidth (HWHM) of the O(2–3) B_{1g} modes at $T=20$ K. Symbols are the same as in (b).

the volume increase around the O(2/3) ions with Pr substitution. A mixing with the apical oxygen ion is also indicated by the similar polarization dependence and resonance profiles of the $\sim$430-cm^{-1} and $\sim$500-cm^{-1} phonons in Y123.[41,42]

Previous studies on mixed $Y_{1-x}Pr_x123$ compounds have shown conflicting results regarding the variation in the O(2/3) B_{1g} phonon frequency and line shape with x; both one-mode[10,12,18] and two-mode[13] behavior has been reported. A recent study by Bogachev *et al.*[19] on $R_{0.5}Pr_{0.5}123$ appears to give convincing evidence for two-mode behavior in samples where the difference in ion radius $\Delta r = r_{Pr} - r_{Re}$ was large, e.g., for R=Y, where the frequency splitting between the ''Y-like'' and ''Pr-like'' modes was found to be $\sim$15 cm^{-1}.

Figure 7(a) shows the change in the spectral region around the O(2/3) B_{1g} phonon with increasing x in $Y_{1-x}Pr_x124$. For intermediate x we find that this frequency region contains three overlapping but well-defined modes in both $Y_{1-x}Pr_x124$ and $Y_{1-x}Pr_x247$. The narrowest ($\Gamma_{HWHM} \approx 3-4$ cm^{-1}) peak is caused by the Cu(1) B_{3g} mode (see Sec. III B 1), while the two broad peaks can be assigned to the O(2/3) B_{1g} mode, which is split into one Y-like and one Pr-like mode.

For $0.2 > x < 0.8$ we found that Gaussian line shapes resulted in significantly better curve fits of the O(2/3) B_{1g} modes than Lorentzian line shapes. This is not surprising, since the random (Gaussian) variation in local Pr concentration should be large in this substitutional range. In the low- and high-substitution regions ($x \leqslant 0.2$, $x \geqslant 0.8$) we find that the majority mode (i.e., the Y-like mode for $x \leqslant 0.2$, etc.) is clearly Lorentzian, as expected. However, the minority mode can be quite well approximated by either line shape, within the experimental accuracy. A fit to a Lorentzian results in a significantly smaller linewidth and integrated intensity, which seems to be physically more reasonable than the Gaussian shape. The position of the minority mode is, however, more or less independent on the choice of line shape. Figures 7(b) and 7(c) summarize the change in frequency and linewidth of the two O(2/3) B_{1g} modes with x. The line widths of both modes, see Fig. 7(c), exhibits a broad maximum for intermediate x as expected. The frequency variation with x is, however, not trivial; both modes exhibit a more or less identical decrease in frequency with x, which results in an almost constant splitting $\omega_Y(x) - \omega_{Pr}(x) \approx 15$ cm^{-1}, i.e., the same splitting as was found in $Y_{0.5}Pr_{0.5}123$ by Bogachev *et al.*[19]

We tentatively interpret the behavior of the O(2/3) B_{1g} modes as the combined effect of (1) a short-range interaction between the O(2/3) and ions close to either Pr or Y and (2) a long-range interaction between the O(2/3) and the average lattice. In this interpretation the splitting between the two modes at a certain x is caused by the difference between the Y-O(2/3) and Pr-O(2/3) force constants, while the frequency decrease with x is caused by the expansion of the average lattice. We note that the frequency dependence in Fig. 7(b) excludes the possibility of the two-mode behavior being the result of long-range phase segregation. If that would have been the case, the Y-like and Pr-like modes would have been centered close to 340 cm^{-1} and 300 cm^{-1}, irrespective of x.

V. SUMMARY AND CONCLUSIONS

We have investigated the phonon Raman spectrum of ceramic $Y_{1-x}Pr_xBa_2Cu_4O_8$ ($Y_{1-x}Pr_x124$) within the full compositional range, as well as $(Y_{1-x}Pr_x)_2Ba_4Cu_7O_{15-\delta}$ ($Y_{1-x}Pr_x247$) with $x=0$–0.6. Data recorded at room temperature and at $T=20$ K are presented. Micro-Raman spectra of crystallites in the nonsuperconducting Pr124 sample show that several phonons display asymmetric Fano line shapes, which are very similar to what has been found in superconducting Y124. The B_{2g}, B_{3g}, and A_g symmetry phonon frequencies vary smoothly with Pr content over the whole compositional range, although the plane-oxygen out-of-phase mode exhibits a two-mode behavior for intermediate doping levels at $T=20$ K. For increasing x, the phonon frequency changes can be understood as the result of an expansion of the ab plane, and the volume around the Y/Pr site, along with a contraction of BaO-layer and CuO double-chain regions along the c axis. There is no evidence for any charge-transfer effects that can be linked to the different rates of T_c suppression with Pr substitution in the three Y-Ba-Cu-O systems.

ACKNOWLEDGMENTS

This work was supported by the Swedish Research Council for Technical Sciences (TFR) and the Swedish Superconductivity Consortium.

[1] H. B. Radousky, J. Mater. Res. **7**, 1917 (1992).
[2] D. P. Norton, D. H. Lowndes, B. C. Sales, J. D. Budai, E. C. Jones, and B. C. Chakoumakos, Phys. Rev. B **49**, 4182 (1994).
[3] R. Fehrenbacher and T. M. Rice, Phys. Rev. B **70**, 3471 (1993).
[4] K. Takenaka, Y. Imanaka, K. Tamasaku, T. Ito, and S. Uchida, Phys. Rev. B **46**, 5833 (1992).
[5] N. Seiji, S. Adachi, and H. Yamauchi, Physica C **227**, 377 (1994).
[6] Y. Yamada, S. Horii, N. Yamada, Z. Guo, Y. Kodama, K. Kawamoto, U. Mizutani, and I. Hirabayashi, Physica C **231**, 131 (1994).
[7] A. Matsushita, Y. Yamada, N. Yamada, S. Horii, and T. Matsumoto, Physica C **242**, 381 (1995).
[8] E. Kaldis, P. Fisher, A. W. Hewat, J. Karpinski, and S. Rusiecki, Physica C **159**, 668 (1989).
[9] M. Kakihana, S.-G. Eriksson, L. Börjesson, L.-G. Johnansson, C. Ström, and M. Käll, Phys. Rev. B **47**, 5359 (1993).
[10] H. B. Radousky, K. F. McCarty, J. L. Peng, and R. N. Shelton, Phys. Rev. B **39**, 12 383 (1989).
[11] H. J. Rosen, R. M. Macfarlane, E. M. Engler, V. Y. Lee, and R. D. Jacowitz, Phys. Rev. B **38**, 2460 (1988).
[12] M. N. Iliev, G. A. Zlateva, P. Nozar, and P. Stastny, Physica C **191**, 477 (1992).
[13] I.-S. Yang, G. Burns, F. H. Dacol, and C. C. Tsuei, Phys. Rev. B **42**, 4240 (1990).
[14] I.-S. Yang, G. Burns, F. H. Dacol, J. F. Bringley, and S. S. Trail, Physica C **171**, 31 (1990).
[15] I.-S. Yang, Y. J. Wee, S.-J. Kim, K. Nahm, C. K. Kim, M. Han, W. C. Yang, and S.-J. Oh, Phys. Rev. B **48**, 7570 (1993).
[16] C. Thomsen, in *Light Scattering in Solids VI*, edited by M. Cardona and G. Güntherodt (Springer, Berlin, 1991).
[17] R. M. Macfarlane, M. C. Krantz, H. J. Rosen, and V. Y. Lee, Physica C **162-164**, 1091 (1989).
[18] K. F. McCarty, J. Z. Liu, Y. X. Jia, R. N. Shelton, and H. B. Radousky, Phys. Rev. B **46**, 11 958 (1992).
[19] G. Bogachev, M. Abrashev, M. Iliev, N. Polulakis, E. Liarokapis, C. Mitros, A. Koufoudakis, and V. Psyharis, Phys. Rev. B **49**, 12 151 (1994).
[20] A. P. Litvinchuk, C. Thomsen, I. E. Trofimov, H.-U. Habermeier, and M. Cardona, Phys. Rev. B **46**, 14 017 (1992).
[21] R. Li, R. Feile, G. Jakob, T. Hahn, and H. Adrian, Phys. Rev. Lett. **70**, 3804 (1993).
[22] K.-M. Ham, R. Sooryakumar, C. Kwon, Q. Li, and T. Venkatesan, Phys. Rev. B **48**, 16 744 (1994).
[23] N. Watanabe, S. Adachi, S. Tajima, H. Yamauchi, and N. Koshizuka, Phys. Rev. B **48**, 4180 (1993).
[24] N. Watanabe, S. Tajima, N. Koshizuka, S. Adachi, N. Seiji, and H. Yamauchi, Physica C **235-240**, 1175 (1994).
[25] M. Kakihana, M. Käll, L. Börjesson, H. Mazaki, H. Yasuoka, P. Berastegui, S. Eriksson, and L.-G. Johannson, Physica C **173**, 377 (1991).
[26] P. Berastegui, M. Kakihana, M. Yoshimura, H. Mazaki, H. Yasuoka, L.-G. Johansson, S. Eriksson, L. Börjesson, and M. Käll, J. Appl. Phys. **73**, 2424 (1993).
[27] P. Berastegui, L.-G. Johansson, M. Käll, and L. Börjesson, Physica C **204**, 147 (1992).
[28] P. Berastegui, L.-G. Johansson, C. Ström, M. Kakihana, and H. Mazaki, Physica C **235-240**, 369 (1994).
[29] E. T. Heyen, R. Liu, C. Thomsen, R. Kremer, M. Cardona, J. Karpinski, E. Kaldis, and S. Rusiecki, Phys. Rev. B **41**, 11 058 (1990).
[30] K. F. McCarty, J. Z. Liu, R. N. Shelton, and H. B. Radousky, Phys. Rev. B **41**, 8792 (1990).
[31] M. Käll, A. P. Litvinchuk, P. Berastegui, L.-G. Johansson, and L. Börjesson, Physica C **225**, 317 (1994).
[32] H. Monien and A. Zawadowski, Phys. Rev. Lett. **63**, 911 (1989).
[33] T. P. Deveraux, A. Virosztek, and A. Zawadowski, Phys. Rev. B **51**, 505 (1995).
[34] E. Sherman, R. Li, and R. Feile, Solid State Commun. (to be published).
[35] R. Feile, R. Li, U. Weimer, C. Tomè-Rosa, and H. Adrian, in *Electronic Properties of High-T_c Superconductors*, edited by H. Kuzmany, M. Mehring, and J. Fink (Springer, Berlin, 1993).
[36] E. Altendorf, X. K. Chen, J. C. Irwin, R. Liang, and W. N. Hardy, Phys. Rev. B **47**, 8140 (1993).
[37] E. T. Heyen, M. Cardona, J. Karpinski, E. Kaldis, and S. Rusiecki, Phys. Rev. B **43**, 12 958 (1991).
[38] D. N. Basov, R. Liang, D. A. Bonn, W. N. Hardy, B. Dabrowski, M. Quijada, D. B. Tanner, J. P. Rice, D. M. Ginsberg, and T. Timusk, Phys. Rev. Lett. **74**, 598 (1995).
[39] J. Humlicek, A. P. Litvinchuk, W. Kress, B. Lederle, C. Thomsen, M. Cardona, H.-U. Harbermeier, I. E. Trofimov, and W. Konig, Physica C **206**, 345 (1993).
[40] Y. T. Ren, Y. Y. Xue, Y. Y. Sun, and C. W. Chu, Physica C **213**, 224 (1993).
[41] E. T. Heyen, S. N. Rashkeev, I. I. Mazin, O. K. Andersen, R. Liu, M. Cardona, and O. Jepsen, Phys. Rev. Lett. **65**, 3048 (1990).
[42] O. V. Misochko, E. I. Rashba, E. Y. Sherman, and V. B. Timofeev, Phys. Rep. **194**, 387 (1991).